

Preparation and characterization of an efficient zeolitic material from a local natural kaolinitic clay and its uses in the elimination of an organic dye

Tahani Achouak Chinar* and Mohammed Benbouzid

Laboratoire des Sciences Analytiques Matériaux et Environnement, Département de Chimie, Université Larbi Ben M'Hidi, 04000, Oum El Bouaghi, Algeria

* Corresponding author at: Laboratoire des Sciences Analytiques Matériaux et Environnement, Département de Chimie, Université Larbi Ben M'Hidi, 04000, Oum El Bouaghi, Algeria.

Tel.: +213.32558609. Fax: +213.32424213. E-mail address: tahani91ach@gmail.com (T.A. Chinar).

ARTICLE INFORMATION



DOI: 10.5155/eurjchem.7.4.410-415.1486

Received: 08 August 2016

Received in revised form: 20 September 2016

Accepted: 25 September 2016

Published online: 31 December 2016

Printed: 31 December 2016

KEYWORDS

Dye
 Adsorption
 Zeolite LTA
 Ion exchange
 Environment
 Kaolinitic clay

ABSTRACT

The zeolitic porous material was prepared from kaolinitic clay (DD1 from Gebel Debbagh, Algeria) using a cheap and easy process to insert a sodium ion into the kaolinitic clay structure. The obtained zeolitic Linde Type-A (LTA) material was characterized by elemental analysis, infrared spectroscopy, thermogravimetric analysis, scanning electron microscopy and X-ray diffraction techniques. The adsorption capacity of the zeolitic porous material was tested with methylene blue. The best correlation of experimental results was obtained with the Langmuir model giving a Q_{max} of 11.5 mg/g indicating a favorable process for the adsorption of the dye.

Cite this: *Eur. J. Chem.* 2016, 7(4), 410-415

1. Introduction

Kaolinitic clay is a low cost natural material and a very versatile mineral that was used in many applications for its adsorption and sieving properties [1-4]. These materials are often complex mixtures of natural minerals with highly variable particle sizes and physicochemical properties [1]. Nowadays, the use of clays, particularly those containing SiO_2 and Al_2O_3 , are experiencing a considerable interest in the industry. Low cost zeolite A with an Al/Si ratio of 1:1 is a major product from thermally activated clay materials containing kaolin or metakaolin [5-7]. Zeolites LTA are more versatile and are widely used in industrial applications such as catalysts, adsorbent, sieving and ion exchanger [1,5,7]. The contamination of waste water with complex carcinogenic aromatic structures in synthetic dyes discharged daily as aqueous waste causes many problems such as toxicity and oxygen demand of the effluent [8,9]. The aim of this work is to synthesize a zeolitic porous material from low cost and local natural kaolinitic clay using a very simple preparative procedure and investigate its effectiveness for the removal of synthetic dyes from aqueous solutions.

2. Experimental

2.1. Materials and reagents

The kaolinitic clay of grade DD1 was obtained from the clay hills in Guelma, Algeria. The sodium hydroxide (99%) was purchased from Aldrich.

2.2. Instrumentation

The methods of analyses used in the characterization of the three materials (kaolinitic clay, metakaolin and zeolitic porous material) are as follows. The UV visible data was recorded using the SHIMADZU dual beam (Kyoto/Japan) UV-Vis spectrophotometer model UV-1601. The FT-IR analyses in the solid phase were recorded using the infrared spectrophotometer (JASCO, FT/IR-4100). For the thermogravimetric analysis (TGA), the tests were performed on a SETARAM equipment type TG-DTA 92-16, mass loss and the formation of the phases of the various samples were measured in air between 30 and 900 °C. The heating rate was constant 10 °C/min. Elemental analyzes were realized using the fluorescence apparatus FLS-QCX system.

Table 1. Elemental analyses of the kaolinitic clay, the metakaolin and the zeolitic LTA form of the clay.

Compounds	% Composition Kaolinitic clay	% Composition Metakaolin form of the clay	% Composition Zeolite LTA form of the clay
SiO ₂	46.792	53.794	46.117
Al ₂ O ₃	38.710	42.589	35.830
Fe ₂ O ₃	0.208	0.302	0.487
CaO	3.463	3.301	3.195
MgO	2.234	2.245	2.202
K ₂ O	0.404	0.349	0.340
Na ₂ O	0.245	0.278	1.991
SO ₂	0.024	0.045	0.107
Cl	0.025	0.023	0.024
Lime saturation factor (LSF)	1.936	1.620	1.836
Silica Modulus (SM)	1.215	1.254	1.270

* LSF = CaO/(2.8SiO₂ + 1.2Al₂O₃ + 0.65Fe₂O₃); SM = SiO₂/(Al₂O₃ + Fe₂O₃).

The X-Ray Diffraction (XRD) analyses were carried out using the STOE STADIP diffractometer provided with a Cu anticathode ($\lambda = 1.542 \text{ \AA}$) with a filter nickel, a divergence slit of 1° and a receiving slit of 0.1 mm. The scanning electronic microscopy (SEM) analyses were achieved using the instrument PHILIPS XL30FEG model.

2.3. Preparation of the zeolitic porous material

The kaolinitic powder (45 μm) was calcined at the temperature of 600 °C for four hours and converted to the metakaolin form [10,11] which was then transferred to a polyethylene flask and treated with an 8 M sodium hydroxide solution in the ratio of 1:5 at the temperature of 90 °C for four hours. The product obtained was washed several times to a neutral pH with distilled water and then filtered and dried for three hours in an oven at the temperature of 110 °C. The zeolitic form of the clay was then formulated into pellets of 4 mm in diameter and 1.6 mm in thickness by mixing it with 15% of the metakaolinitic clay and 30% of distilled water. The pellets obtained were dried at 80 °C in an oven for three hours and then calcined at 400 °C for four hours. The pellets obtained were used for the removal of the dyes.

2.4. Adsorption tests

Adsorption experiments were conducted at the temperature of 20 °C in a batch mode. The various tests for the study of the adsorption isotherms were carried out on electromagnetic stirrers (1200 rpm) in a series of conical flasks of 25 mL. The zeolitic porous material (0.03 g) was added each time to the contact solution (30 mL) containing the test compound at a constant initial concentration C_0 (12 mg/L) of methylene blue (MB). All flasks were placed on a magnetic stirrer when determining the contact time. The flask contents were then centrifuged and the supernatant were analyzed by UV-Visible at the appropriate maximum wavelength ($\lambda_{\text{max}} = 663 \text{ nm}$). The adsorption equilibrium time corresponds to the plateau portion of the curve where the maximum adsorption is reached.

2.5. Effect of contact time

The contact time between the adsorbate and the adsorber is of significant importance in the treatment of wastewater by adsorption [12]. The measurements were carried out to monitor changes in the concentration of methylene blue as a function of time and determine the time required for the equilibrium to take place in the mixture methylene blue/zeolitic clay.

3. Results and discussion

3.1. Characterizations

3.1.1. Qualitative and quantitative elemental analysis

The results of the chemical analyzes of the three samples are shown in Table 1. The elemental analysis showed that the three samples (kaolinitic clay, metakaolin form of the clay, zeolitic LTA form of the clay) rich in SiO₂ and Al₂O₃ are aluminosilicate materials.

3.1.2. X-ray diffraction analysis

The values ' d ' of the interplanar spacing obtained, are compared to those of the International Centre for Diffraction Data (ICDD) files and allowed to highlight the various existing phases. The powder X-ray diffraction pattern showed a major diffraction of the zeolitic porous material. It showed also that the product comprises also a proportion that consists of the metakaolin (introduced during the formulation of the pellets) and some quartz (Figure 1).

3.1.3. FT-IR analysis

The different IR absorptions of the materials (kaolinitic clay, metakaolin to the zeolitic LTA form of the clay) are clearly observed in the region (400-4000 cm^{-1}). It showed that the presence of functional groups of the type: T-O-T, T-O, T-O-H (where T may be Si or Al). The kaolinitic clay material gave well-defined absorption bands located at: 469.58, 790.67, 912.16 and 1034.62 cm^{-1} which are characteristic of Si-O deformations of the Si-O-Al and the Al-OH and Si-OH vibrations respectively (Figure 2a). This is consistent with the literature [12-14]. The FT-IR of the zeolitic porous material showed the appearance of the following absorption bands at 462.83 cm^{-1} corresponding to the TO vibrations; 546.72 cm^{-1} which corresponds to the vibrations of the skeleton TOT and 1034.62 cm^{-1} which corresponds to the Si-OH vibrations, and they are consistent with the literature [11] (Figure 2b). The broad absorption in the region of 1650 cm^{-1} corresponds to the O-H deformation of the water and the broad absorption between 3200 and 3700 cm^{-1} also characterizes the OH groups.

3.1.4. Thermogravimetric analysis (TGA)

The kaolinitic clay showed a gradual and a relatively rapid and gradual loss of weight (Figure 3a). The TGA for this material showed a loss of weight between 0 and 550 °C which reached a top speed at 518 °C and then stabilized at 600 °C. This can be explained by the dehydroxylation first and then by the thermal decomposition of the kaolinitic clay and the formation of the Al-Si phase. The TGA of the zeolitic LTA form of the clay showed a gradual loss of weight which was relatively fast (Figure 3b). The weight continually decreased up to the temperature of 900 °C. An inflection point was observed at 450 °C which corresponds to a weight loss of 13.5%. The TGA of the zeolitic LTA form of the clay indicated the presence of a single main phase of Al-Si which appeared at around 500 °C.

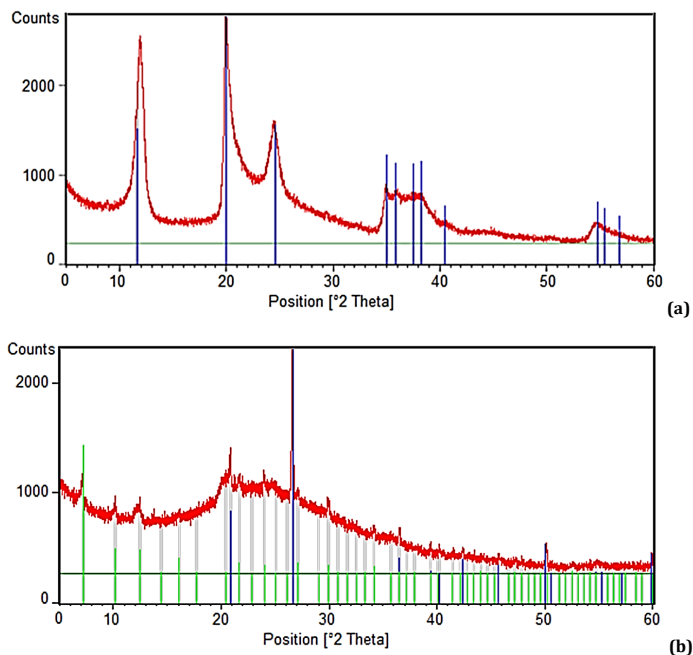


Figure 1. XRD analysis of (a) the kaolinitic clay and (b) the zeolitic porous material.

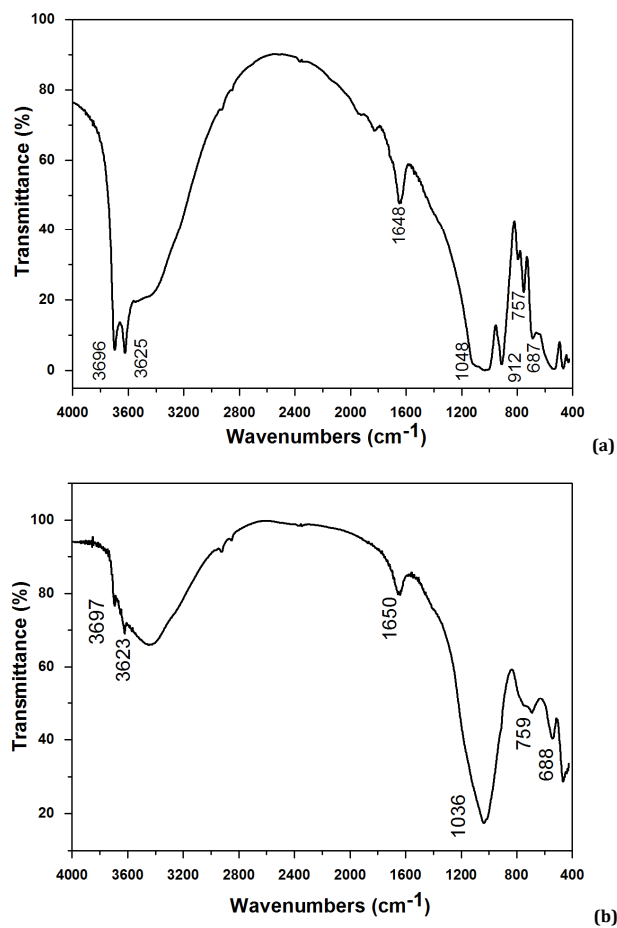


Figure 2. Infrared spectrum of (a) the kaolinitic clay and (b) the zeolitic porous material.

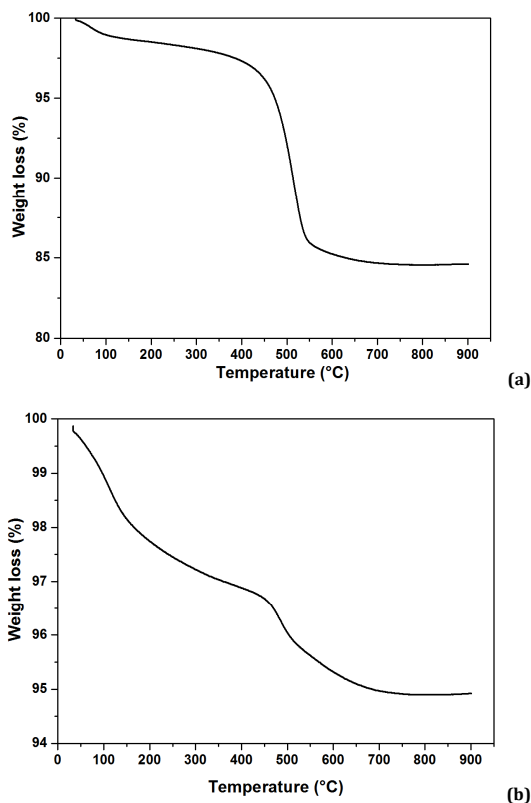


Figure 3. TGA of (a) kaolinitic clay and (b) the zeolitic LTA form of the clay.

3.1.5. SEM analysis

The scanning electronic microscopy (SEM) analysis of the kaolinitic clay material showed crystals of acicular form with variable sizes having a maximum length of 1 micron (Figure 4). The SEM analysis of the zeolitic LTA form of the clay showed the presence of large crystals of faceted cubic form, (1-2 microns) representing the zeolite LTA and small crystals of what could be the metakaolinitic form used to prepare the pellets.

3.2. Determination of the adsorption equilibrium of the dye onto the zeolitic LTA form of the clay

Figures 5a and 5b show the methylene blue removal rate. In the first minutes, the adsorption process of the dye was extremely fast. It can be explained by the abundant availability of active sites (pores) on the surface of the zeolitic LTA form of the clay during this first period. After that, the adsorption was slower and remained almost unchanged which corresponds to equilibrium since all sites became occupied. It is concluded that under these conditions the optimum contact time required for the methylene blue (MB) dye solutions to reach equilibrium was 45 minutes.

3.3. Adsorption isotherm studies

The experimental equilibrium data were fitted using three isotherm models as Langmuir isotherm, Freundlich isotherm and Temkin isotherm.

3.3.1. Langmuir isotherm

The Langmuir model assumes a uniform surface where there is no interaction between adsorbed molecules [15]. The linear expression of the Langmuir model used as;

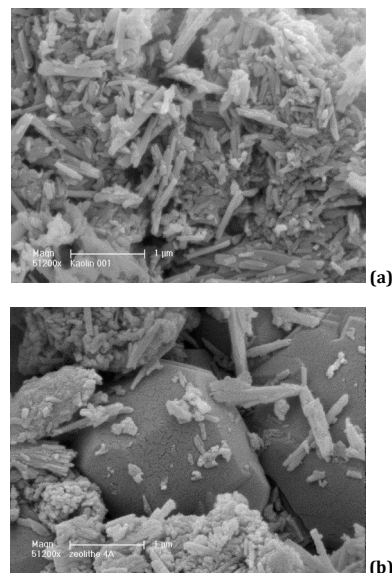


Figure 4. Scanning electronic microscopy (SEM) analysis of (a) kaolinitic clay and (b) the zeolitic form of clay.

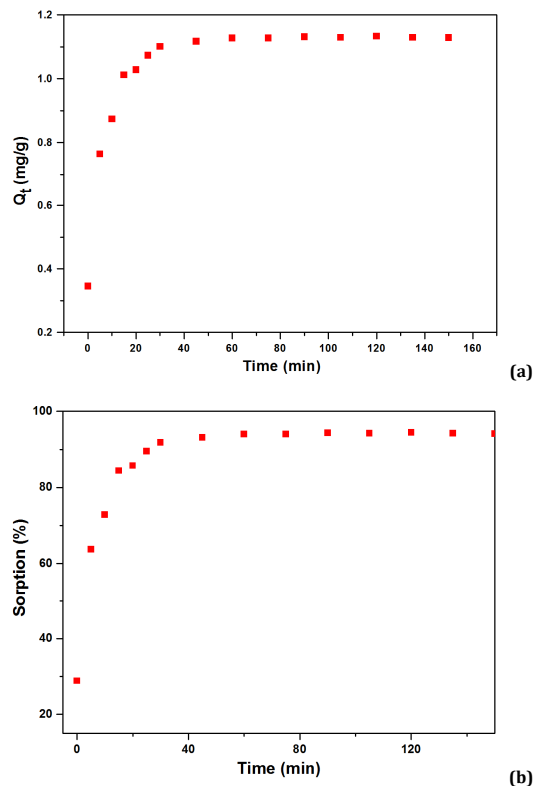


Figure 5. a) Effect of contact time on the concentration of methylene blue on the zeolitic porous material at the temperature of 20 °C and $C_0 = 12$ mg/L, b) Percentage sorption of methylene blue on the zeolitic porous material versus time at the temperature of 20 °C and $C_0 = 12$ mg/L.

$$C_e/q_e = C_e/q_{\max} + 1/q_{\max} \cdot K_L \quad (1)$$

where, C_e is the concentration of the dye in solution (mg/L) at equilibrium with the adsorbed dye, q_e is the amount of the adsorbed dye (mg/g) at the solid/liquid interface, q_{\max} is the

monolayer capacity of the adsorbent (mg/g), KL is the Langmuir adsorption constant (L/mg).

The adsorption isotherm of the adsorption of methylene blue (MB) on the zeolitic porous material is shown in Figure 6.

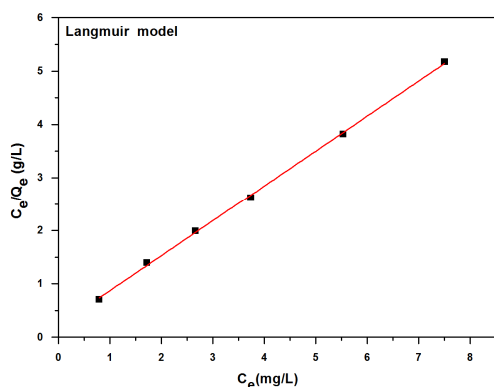


Figure 6. Plot of the Langmuir model for the adsorption of methylene blue (MB) on the zeolitic porous material at the temperature of 20 °C.

3.3.2. Freundlich isotherm

The Freundlich model assumes multilayer reversible sorption on heterogeneous surface [16]. The Freundlich expression is represented by the following linear equation:

$$\log q_e = \log K_F + (1/n) \cdot \log C_e \quad (2)$$

where, C_e is the concentration of the dye in solution (mg/L) at equilibrium with the adsorbed dye, q_e is the amount of the adsorbed dye (mg/g) at the solid/liquid interface, K_F and $1/n$ are empirical parameters, K_F is the adsorption constant related to the bonding energy and $1/n$ is associated to the surface heterogeneity.

The adsorption isotherm of the adsorption of methylene blue (MB) on the zeolitic porous material is shown in Figure 7.

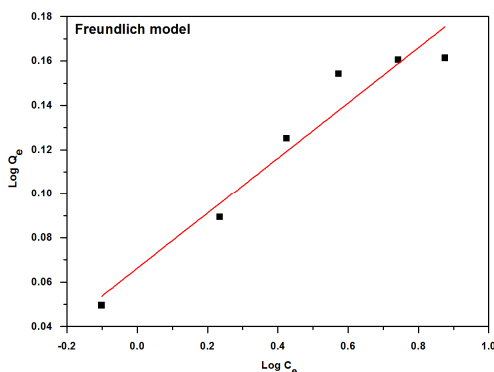


Figure 7. Plot of the Freundlich model for the adsorption of methylene blue (MB) on the zeolitic porous material at the temperature of 20 °C.

3.3.3. Temkin isotherm

The Temkin model considers the adsorbate-adsorbent interaction and assumes that the sorption heat reduces linearly with surface coverage [17]. The Temkin model is described by the following linear equation:

$$q_e = B \ln A_T + B \ln C_e \quad (3)$$

where A_T (L/g) is the equilibrium binding constant, corresponding to the maximum binding energy, and constant

B is related to the heat of adsorption. A plot of q_e versus $\ln C_e$ enables the determination of the isotherm constants B and A_T from the slope and intercept of the straight line plot.

The adsorption isotherm of the adsorption of methylene blue (MB) on the zeolitic porous material is shown in Figure 8.

Figures 6-8 represent the adsorption isotherm of Langmuir ($r^2 = 0.999$), Freundlich ($r^2 = 0.932$) and Temkin ($r^2 = 0.935$) for the adsorption of MB on the zeolitic porous material prepared. Since the best correlation factor for the experimental results were found in the Langmuir model, this model fits better the equilibrium data. The maximum adsorption capacity for MB deduced from this model was $Q_{max} = 11.5$ mg/g.

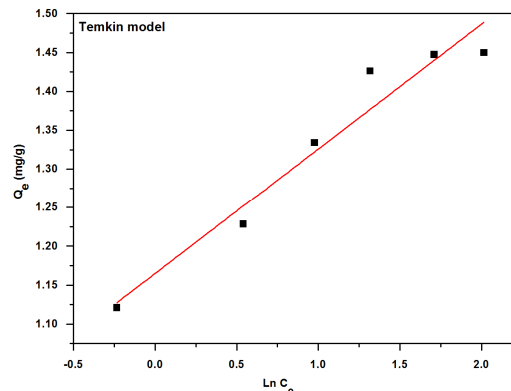


Figure 8. Plot of the Temkin model for the adsorption of methylene blue on the zeolitic porous material at the temperature of 20 °C.

4. Conclusion

The work presented in this study describes all the steps involved in the preparation of the zeolitic LTA form of the clay from a local kaolinitic clay, its characterization with different methods of analysis and its use as a decontaminating material. This preparation resulted in a more efficient low cost renewable and environmentally friendly material with a Q_{max} of 11.5 mg/g comparable to the adsorption of some zeolites and modified zeolites [18] and better than the adsorption of some kaolinitic materials [19]. The prepared material can also be regenerated [20-22].

Acknowledgement

The authors gratefully acknowledge the support provided by Professor Saïd Benfarhi from Lhadj Lakhdhar University Batna (Algeria), Professor Jean Louis Paillaud from Haute Alsace University (France), the company SCIMAT (Société des Ciments de Ain-Touta, Algeria) and the company CETIM (Centre d'Etude et de Services Technologiques de l'Industrie des Matériaux) Boumerdes, Algeria.

References

- [1]. Murray, H. H. *Appl. Clay Sci.* **1991**, *5*, 379-395.
- [2]. Vatan, A.; Manuel de Sédimentologie, Editions Technip, Paris, 1967, pp. 383-385.
- [3]. Volzone, C.; Gallegos, N.; Cantera C.; Greco, A. *Eur. J. Chem.* **2013**, *4(4)*, 366-369.
- [4]. Kandil, A. E. H. T.; Saad, E. A.; Aziz, A. A. A.; Aboelhasan, A. E. *Eur. J. Chem.* **2012**, *3(1)*, 99-105.
- [5]. Deepak, A.; Alan, C.; Howe, R. F. *Micropor. Mesopor. Mat.* **1997**, *19*, 359-365.
- [6]. Vilma, S.; Ursula, K.; Ruby, C. *J. Chem. Technol. Biot.* **1999**, *74*, 358-363.
- [7]. Lin, D. C.; Xu, X. W.; Zuo, F.; Long, Y. C. *Micropor. Mesopor. Mat.* **2004**, *70*, 63-70.
- [8]. El-Mekki, D. M.; Ibrahim, F. A.; Selim, M. M. *J. Environ. Chem. Eng.* **2016**, *4*, 1417-1422.
- [9]. Ozer, D.; Dursun, G.; Ozer, A. *J. Hazard. Mater.* **2007**, *144*, 171-179.

- [10]. Prokof'ev, V.Y.; Gordina, N.E. *Appl. Clay Sci.* **2014**, *101*, 44-51.
- [11]. Ugal, J. R.; Hassan, K. H.; Ali, I. H. *J. Assn. Arab. Univ. Basic Appl. Sci.* **2010**, *9*, 2-5.
- [12]. Dogan, M.; Ozdemir, Y.; Alkan, M. *Dye Pigments* **2007**, *75*, 701-713.
- [13]. Loiola, A.R.; Andrade, J.C.R.A.; Sasaki, J.M.; da Silva, L.R.D. *J. Colloid Interf. Sci.* **2012**, *367*, 34-39.
- [14]. Salem, A.; Akbari Sene, R. *Chem. Eng. J.* **2011**, *174*, 619-628.
- [15]. Langmuir, I. *J. Am. Chem. Soc.* **1918**, *40*, 1361-1403.
- [16]. Freundlich, H.M.F. *J. Phys. Chem.* **1906**, *57*, 385-470.
- [17]. Temkin M.J; Pyzhev, V. *Actaphysiochim. URSS* **1940**, *12*, 217-222.
- [18]. Jin, X.; Jiang, M.; Shan, X.; Pei, Z.; Chen, Z. *J. Colloid Interf. Sci.* **2008**, *328*, 243-247.
- [19]. Ghosh, D.; Bhattacharyya, K.G. *Appl. Clay Sci.* **2002**, *20*, 295-300.
- [20]. Sun, Z.; Li, C. J.; Wu, D. *J. Chemi. Technol. Biot.* **2010**, *85* (6), 845-850.
- [21]. Perego, C.; Bagatin, R.; Tagliabue, M.; Vignola, R. *Micropor. Mesopor. Mater.* **2013**, *166*, 37-49.
- [22]. Purkait, M. K; Maiti, A.; DasGupta, S.; De, S. *J. Hazard. Mater.* **2007**, *145*, 287-295.